Measuring Air Quality in City Areas by Vehicular Wireless Sensor Networks

Shu-Chiung Hu, You-Chiun Wang, Chiuan-Yu Huang, and Yu-Chee Tseng

Abstract—The paper considers a *micro-climate monitoring* scenario, which usually requires deploying a large number of sensor nodes to capture the environmental information. By exploiting *vehicular sensor networks (VSNs)*, it is possible to equip fewer nodes on cars to achieve fine-grained monitoring, because when a car is moving, it could conduct measurements at different locations. Therefore, this paper proposes a VSN architecture to collect and measure the air quality for micro-climate monitoring in city areas, where nodes' mobility may be uncontrollable (such as taxis). In the proposed VSN architecture, we address two network-related issues: 1) how to adaptively adjust the reporting rates of mobile nodes to satisfy a target monitoring quality with less communication overhead and 2) how to exploit the opportunistic communication to reduce message transmissions. We propose some algorithms to solve the two issues and verify their performances by simulations. In addition, we also develop the prototype of a ZigBee-based car network to monitor the concentration of *carbon dioxide (CO_2)* gas in city areas, where the real-test results are reported on the Google Maps.

Index Terms—micro-climate monitoring, opportunistic communication, pervasive computing, vehicular sensor network, wireless sensor network.

1 Introduction

After the industrial revolution, the burning of fossil fuels and a huge number of human activities have significantly increased the concentration of *carbon dioxide (CO_2)* year by year. It is widely concluded that the increase of the CO_2 concentration is a major reason to cause global warming. Therefore, it would be quite interesting to understand how the CO_2 concentration changes over temporal and spatial domains at a very fine-grained size. This is generally related to *micro-climate monitoring*, which means to collect the environmental information in a quite small scale (for example, one measurement per ten meters).

In this paper, we aim at micro-climate monitoring in city areas by using *vehicular sensor networks (VSNs)*. We consider sensor nodes whose mobility may be uncontrolled (for example, equipping sensor nodes on taxis or buses). Micro-level monitoring usually requires deploying a large number of sensor nodes. However, through mobility, a sensor node can conduct measurements at many different locations, thereby relaxing the demands on the number of sensor nodes. Still, this problem poses several challenges: 1) calibration of sensing data, 2) management and operation of VSNs, 3) collection and presentation of the sensing data.

Among the above challenges, we would like to particularly address two *network-related* issues: 1) how to adaptively adjust the reporting rates of mobile nodes to satisfy a target monitoring quality while reducing the communication overhead and 2) how to exploit the opportunistic communication to reduce message transmissions. For example, in a crowded area with many cars carrying sensor nodes, we can reduce the reporting rate of each node to reduce possible duplication. On the other hand, at those fields where the CO_2 concentration changes dramatically, a node may need to increase its reporting rate to improve the accuracy. For the opportunistic communication, a node may pass its sensing data to a neighbor which is going to submit a report shortly. Also, a node which just arrives at an area may inquire of a neighbor (instead of the central server) the required reporting rate inside the area.

We propose a VSN architecture to measure air quality for micro-climate monitoring in city areas, where the CO_2 concentration may change dramatically and the number of sensor nodes could be large. We design two message-efficient algorithms to address issue 1). In particular, the sensing field is divided into regular grids. Each grid imposes its own reporting rate to the nodes inside the grid. The first algorithm tries to measure the changes of the CO_2 concentration inside a grid and then determine the number of reports to be shared by each node. On the other hand, the second algorithm tries to use the changes of the CO_2 concentration and the number of cars inside a grid to determine the new reporting rate. To address issue 2), we allow a node to collect information and submit reports by taking advantage of its neighbors opportunistically.

We verify our results through simulations as well as a real prototype. Specifically, we develop a ZigBee-based car network to monitor the CO_2 concentration in the Hsinchu City, Taiwan, where over 100,000 people commute daily to work. In our prototype, a car is equipped with a CO_2 sensor, a GPS (global positioning system) receiver, and a GSM (global system for mobile communications) module, which form a ZigBee-based intra-vehicle wireless network. These vehicular nodes roam inside the area of interest and periodically report their sensed data through GSM short messages. These reports are collected by a central server, which adopts the Google Maps [1] to demonstrate the monitoring result.

The rest of this paper is organized as follows. Section 2 surveys related work. Section 3 presents the proposed VSN architecture and our algorithms. Section 4 gives the simulation results. The prototyping experiences are presented in Section 5. Section 6 concludes this paper.

S.-C. Hu, C.-Y. Huang, and Y.-C. Tseng are with the Department of Computer Science, National Chiao-Tung University, Hsin-Chu, 30010, Taiwan.
E-mail: {schu, chiuanyu, yctseng}@cs.nctu.edu.tw
Y.-C. Wang is with the Department of Computer Science and Engineering, National Sun Yat-sen University, Kaohsiung, 80424, Taiwan
E-mail: ycwang@cse.nsysu.edu.tw

2 Related Work

Wireless sensor networks (WSNs) have been widely adopted in surveillance and monitoring applications. For example, the work of [2] adopts WSNs to provide a safe and secret way for acquiring the information from hostile targets in military surveillance missions. The OceanSense project [3] deploys a submarine WSN to collect oceanic data such as temperatures and sea depths, while the work of [4] deploys an underground WSN to monitor coal mines. To forecast volcano eruptions, the studies of [5], [6] deploy refractory sensors around active volcanos. WSNs are also deployed to monitor civil infrastructures such as buildings and railway bridges [7], [8]. In addition, the studies of [9], [10] propose multi-layer WSNs to improve the network bandwidth and reduce the energy consumption under various surveillance applications. Therefore, WSNs offer a convenient way to monitor physical environments. However, a large number of sensor nodes need to be deployed in the monitored area, and it is usually difficult to replace or recharge nodes after deployment.

To address the above issues, the mobility concept is introduced to WSNs to dispatch sensor nodes to conduct many missions such as replacing broken nodes or reacting to events [11], [12]. Such WSNs are usually called *mobile WSNs*. Mobility makes sensor nodes more maneuverable and thus mobile WSNs are also adopted in various surveillance applications. For example, iMouse [13] develops a hybrid WSN consisting of static and mobile sensors for indoor surveillance, where mobile sensors with more powerful computation and sensing capability are dispatched to analyze the abnormal events reported from static sensors. SensorFlock [14], an airborne WSN composed of various micro-aerial sensing devices, is designed to analyze toxic plume and storm dynamics to build a three-dimensional view of the atmospheric system. ZebraNet [15] is developed to track zebras' migration in Africa, where sensor nodes are equipped on zebras to record their movement and interaction. It can be observed that in the above systems, sensor nodes should be equipped on either specially-made mobile carrier or animals.

Several studies suggest adopting common vehicles such as cars and bicycles as the mobile carriers of sensor nodes to reduce the deployment cost. For example, by equipping multiple types of sensor nodes such as microphones and cameras on bicycles, the work of [16] allows cyclists to ride these bicycles to collect the road information along some predefined routes. In the work of [17], cars are equipped with vehicular sensors and GPS receivers to conduct car-health monitoring and driver characterization. The work of [18] equips cameras and chemical sensors on vehicles to monitor pollution along streets, where vehicles may exchange their monitoring data when they meet each other. In CarTel [19], each car is equipped with a GPS receiver to trace its route, a camera to monitor road conditions, and a wireless interface to report data to a central server. These reports can be used for future route planning. Compared with the above studies, our work not only develops a VSN architecture for micro-climate monitoring in city areas but also addresses two network-related issues. Different from [16], [17], [19], we aim at adaptively adjusting the reporting rates of vehicles to balance between the monitoring accuracy and the monetary cost. Note that a higher reporting rate improves the monitoring accuracy but burdens users with a high cost (because they need to send more GSM messages), and vice versa. There, our goal is to satisfy a target monitoring quality with less communication overhead. In addition, we exploit the opportunistic communication to aggregate vehicles' reports to further reduce the overall message transmission in our VSN architecture.

3 VSN-Based Solutions for Micro-climate Monitoring

Fig. 1 shows the proposed VSN architecture for micro-climate monitoring. The architecture is composed of a few number of vehicular sensor nodes, a monitoring server, and cellular networks. Each vehicular sensor node (or simply called *vehicular node* or *node*) consists of a central unit and an external unit. The central unit is connected to a cellular interface (for example, 2G/3G/3.5G), a GPS receiver, and wireless interfaces. The external unit is connected to a wireless interface and some sensors specified by the target application. Here, we consider monitoring the CO_2 concentration, so a CO_2 sensing device is adopted. The central and external units communicate with each other through their wireless interfaces (in this paper we adopt ZigBee). Periodically, the central unit collects the detected CO_2 concentration from the external unit and reports the data, together with its current location, to the monitoring server. The monitoring server then collects all data in each predefined time frame and renders the result on a map (in this paper we adopt the Google Maps).

To reduce the loads on cellular networks and improve the communication efficiency, the central unit of a vehicular node can also form an ad hoc network with nearby nodes via their wireless interfaces (for example, Wi-Fi) to relay sensing reports for others. Specifically, such ad hoc networks would allow the opportunistic communication among vehicular nodes. Therefore, a node can collect new information from its neighbors and help relay other nodes' sensing data to the monitoring server.

In this paper, we consider two network-related issues in the micro-climate monitoring problem. First, since a city area is considered, not only the CO_2 concentration but also the density of vehicular nodes may change dramatically from time to time. Thus, one may need to impose different reporting rates for mobile nodes in different subareas. We call this the *dynamic reporting rate (DRR) problem*, whose goal is to reduce the communication overhead on the cellular networks while achieving certain monitoring quality. Second, to further reduce the reporting overhead, we consider the possibility of the opportunistic communication. When nodes help relay each other's reports, some sort of data aggregation can be achieved. We assume that each report has a time constraint by which it has to be submitted to the server so as to provide timely services. We call this the *time-constrained opportunistic relay (TOR) problem*.

To achieve our goals, the whole sensing field is partitioned into fixed-size grids G_1, G_2, $\ldots$, G_n. For the DRR problem, the monitoring server will impose a reporting rate r_i on all vehicular nodes in grid G_i, $i = 1..n$. For the TOR problem, nodes will find out their reporting rates and submit their reports in an opportunistic manner. The monitoring server has a predefined time frame of T seconds. In every T seconds, the server combines all reports that it has collected during that frame and renders the result on a map interface. Below, we present our detailed solutions.

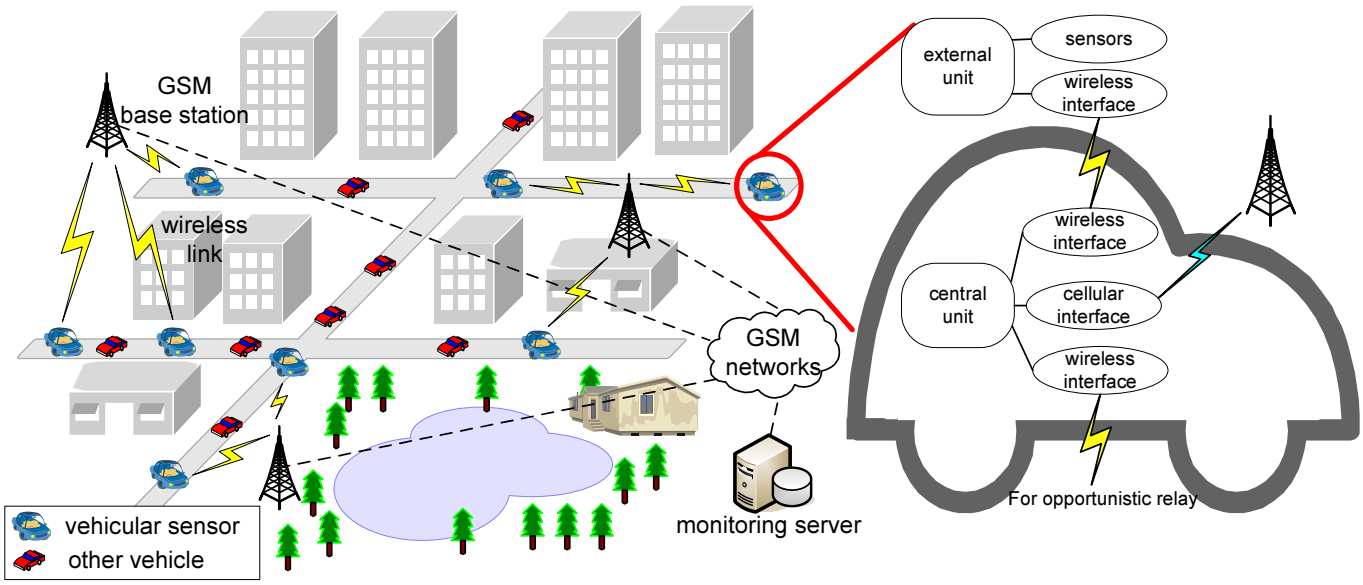

Fig. 1: The proposed VSN architecture for micro-climate monitoring.

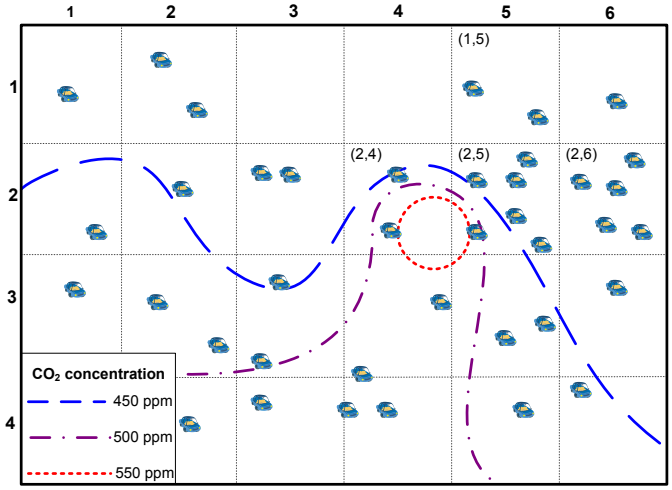

Fig. 2: An example of adjusting the reporting rates in grids.

3.1 Solutions to the DRR Problem

Since the CO_2 concentration is dynamic, we need to decide how many samples we expect to collect from each grid in every time frame based on the record of the previous time frame. The number of samples that we need to collect, however, depends on two factors: 1) the distribution of the CO_2 concentration in the area and 2) the number and the distribution of vehicular nodes in the area. Assuming the target grid to be G_i, we present two schemes below.

3.1.1 Variation-based Scheme

Intuitively, a higher reporting rate r_i should be set when the variation of the CO_2 concentration becomes higher, and vice versa. For example, in Fig. 2, since the CO_2 concentration in grids (2, 4) and (2, 5) fluctuates more quickly than that in other grids, higher reporting rates should be imposed on these two grids. Contrarily, the CO_2 concentration in grids (1, 5) and (2, 6) is flatter, so lower reporting rates could be applied to reduce the amount of transmissions.

From the previous time frame, we can calculate the standard deviation σ_i^{con} of all CO_2 concentration reported from G_i and the number of vehicular nodes v_i that have submitted reports for G_i. We use σ_i^{con} as an index to estimate the number of samples (denoted by S_i^{var}) that we expect to receive in the upcoming time frame. We suggest setting S_i^{var} as a linear function of σ_i^{con}:

$$S_i^{var} = a_i^{var} \times \sigma_i^{con} + b_i^{var},$$

where a_i^{var} and b_i^{var} are constants based on the past experience (larger values mean higher monitoring qualities). Note that b_i^{var} indicates the smallest number of reports that we expect to receive. Then, the new reporting rate of G_i can be set to $r_i^{var} = S_i^{var}/v_i$.

3.1.2 Gradient-based Scheme

The previous variation-based scheme has no sense of the locations where samples are collected (that is, two samples collected from different locations of the grid are regarded as the same). For example, for two samples with a fixed amount of concentration difference, if these two samples are taken at very close locations, the drop of concentration is regarded as more significant than the fluctuation of concentration taken at two farther-away locations. Therefore, the concept of "gradient" can be applied to reflect the above factor.

In this scheme, we collect some high-value and low-value samples and then measure the gradients of all pairs of samples between these two sets. Then, the average gradient is adopted to calculate the new reporting rate. Specifically, let $R_{\max}$ and $R_{\min}$ be the sets of the top $\gamma\%$ and the bottom $\gamma\%$ of concentration readings in G_i in the previous time frame, respectively. The gradient of two samples $x \in R_{\max}$ and $y \in R_{\min}$ can be written as

$$\alpha(x, y) = \frac{x - y}{dist(x, y)},$$

where $dist(x, y)$ is the distance between the two locations where x and y are sampled. Then, the average gradient between $R_{\max}$ and $R_{\min}$ is measured as

$$\alpha_i^{avg} = \frac{\sum_{x \in R_{\max}, y \in R_{\min}} \alpha(x, y)}{|R_{\max}| \times |R_{\min}|}.$$

Similar to the variation-based scheme, the number of samples S_i^{gra} that we expect to receive in the next time frame can be set as a linear function of α_i^{avg}:

$$S_i^{gra} = a_i^{gra} \times \alpha_i^{avg} + b_i^{gra},$$

where a_i^{gra} and b_i^{gra} are constants based on the past experience. Then, the new reporting rate of G_i can be set to $r_i^{gra} = S_i^{gra}/v_i$.

3.2 Solutions to the TOR Problem

Through the opportunistic communication, a vehicular node can inquire the information of reporting rate when it enters a new grid, helps relay others' reports, and estimates its own location when it loses the GPS signal. Our design also includes a randomness mechanism to ensure fairness among nodes when they decide their relaying roles. Note that since GPS is adopted, we assume that nodes are at least roughly time-synchronized. Also, we assume that each node knows the parameter T and the due time when the server will render the monitoring result. The details of our solution are listed below:

- Periodically, a node x broadcasts a HELLO packet, through its wireless interface, which contains its current grid ID and its current attraction value att_x, where

  $$att_x = rnd_x \times wgt_x,$$

  where rnd_x is a random number between 0 and 1 generated by x at the beginning of the current time frame and wgt_x is x's weight variable reflecting the number of sensing reports that x needs to submit to the server so far. Note that wgt_x includes the sensing reports generated by x itself and those that x needs to relay for other nodes.
- When a node does not know the reporting rate of its current grid (either due to node mobility or time movement), it first tries to get this information from any neighbor, if possible, through its wireless interface. When the above opportunistic communication is impossible, the node inquires the server through its cellular interface. Then, according to the reporting rate, the node will collect sensing data from its external unit periodically.
- When a node x finds a neighbor y such that $wgt_x < wgt_y$, it tries to send all sensing reports at its hand to y through its wireless interface. On completion of the above operation, x clears wgt_x to zero. On the other hands, y increases its weight wgt_y by wgt_x. If only part of the above process is done before the link between x and y breaks, then these weights are adjusted proportionally. Note that this step may be extended to multi-hop transferring. However, to reduce complexity and to avoid the ping-pong effect, we choose to only allow one-hop transferring.
- When x finds that it loses the GPS signal (for example, due to signal blocking), it can estimate its current location through its neighbors' locations. (Note that there are several possibilities [20], [21] to conduct such an estimation. This is related to localization and is out of the scope of this paper.)
- After the current time frame ends, each node which has a non-zero weight submits all sensing reports at its hand to the server.

Note that a benefit in the above relaying behavior is the effect of data aggregation. When aggregating multiple sensing reports together, the message volume can be reduced. The reduction ratio is, however, system- and application-dependent. Data aggregation does not affect the measurement accuracy because the server would actually receive the same sensing reports coming from different cars; instead, it would decrease the monetary cost due to message reduction.

4 Simulation Results

We develop a simulator to verify the performances of the proposed algorithms in C++ and Matlab. Table 1 lists the default parameters in our simulator. Specifically, the monitored region is modeled by a 12.8 km $\times$ 12.8 km rectangle, inside which there are 20 horizontal and vertical streets. To simulate a real-road model, vehicular nodes move inside the region following the Manhattan mobility model [22], where all nodes move along horizontal or vertical streets. When meeting an intersection, each vehicular node determines its moving direction following some probabilities. In particular, we set the probabilities that a vehicular node goes straight, turns left, and turns right to 0.5, 0.25, and 0.25, respectively. To keep the total number of vehicular nodes in the monitored region to be constant, we do not allow vehicular nodes to move outside the region. Therefore, when a vehicular node reaches the region's boundary, it will turn to an available direction. Also, each vehicular node knows its current grid by using GPS, and sends its reports by GSM short messages. The length of a GSM short message is set to 140 bytes and charged by one dollar. The monitored region is divided into 4×4 grids. There are several CO_2 events in the monitored region. The occurrence of CO_2 events follows the Gaussian distribution and each event has different lifetime. The rate of the CO_2 concentration variation is defined by the number of CO_2 events generated during 600 seconds. The server has a predefined time frame T, which is set to 600 seconds, to collect messages. (We will also observe the effect of T in the simulations.) We measure the GSM cost and the estimated error of the CO_2 concentration.

For comparison, we develop two schemes which always use the *maximum* and *minimum* reporting rates, where each vehicular node reports its data every 30 and 300 seconds, respectively. Such two schemes are also adopted in [10], [15], where nodes report their data regularly.

We first observe the effect of different numbers of vehicular nodes on the average GSM cost per time frame T and the estimated error, as shown in Fig. 3. The number of vehicular nodes is ranged from 32 to 640. The unit of the estimated error is *parts per million (ppm)*. Explicitly, the number of received messages (and thus the GSM cost) increases while the estimated error decreases. The scheme of maximum reporting rate incurs the most expensive cost because each vehicular node needs to report its data very frequently. On the other hand, the scheme of minimum reporting rate incurs the maximum estimated error because the monitoring server may not collect sufficient data to calculate the CO_2 concentration. Both our variation-based and gradient-based schemes can increase the estimated accuracy while reducing the number of reporting messages. Therefore, the GSM cost can be lowered down. By adopting the gradient concept, the gradient-based scheme can further reduce message transmissions with the expenditure of increasing a small amount of the estimated error.

TABLE 1: The default parameters in our simulators.

parameter	value
the number of streets	20
the area of the monitored region	12.8 km × 12.8 km
the number of grids	16
the number of vehicular nodes	160
the velocity range of vehicular nodes	30∼60 km/hr
the rate of CO_2 variation	2 CO_2 events
the maximum reporting rate	report every 30 seconds
the minimum reporting rate	report every 300 seconds
the time frame T	600 seconds
the length of a GSM short message	140 bytes
the charge fee to send a GSM short message	1 dollar

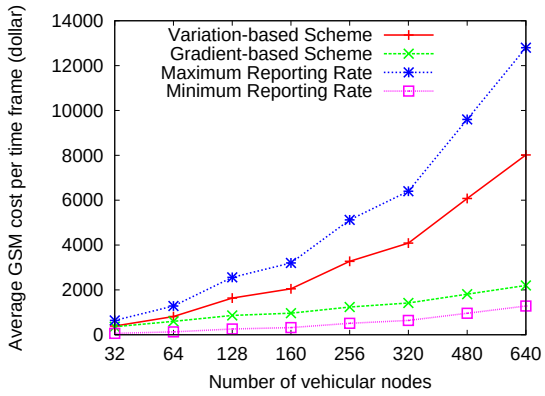

(a) GSM cost

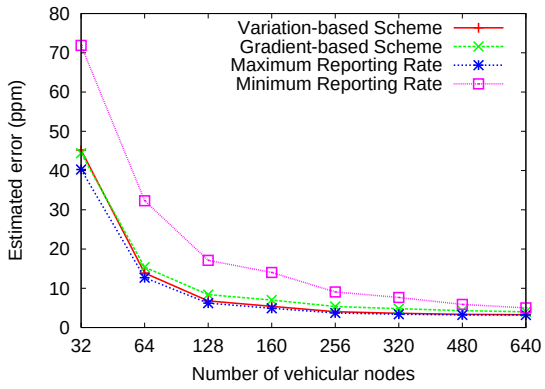

(b) estimated error

Fig. 3: Comparison of the average GSM short message cost per time frame T and the estimated error of the CO_2 concentration under different numbers of vehicular nodes.

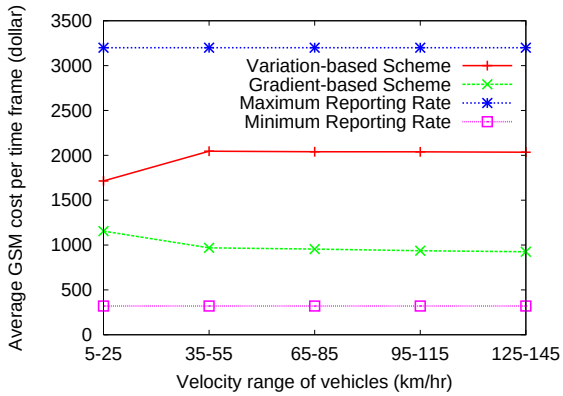

(a) GSM cost

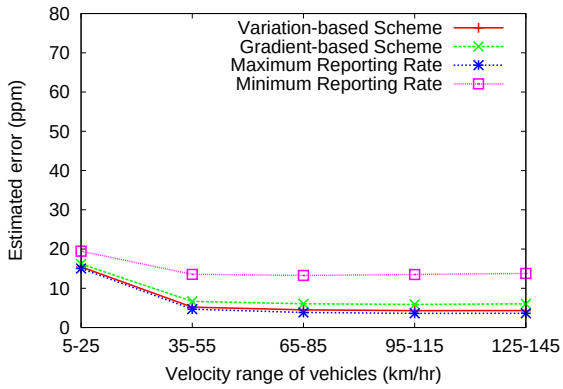

(b) estimated error

Fig. 4: Comparison of the GSM short message cost per time frame T and the estimated error of the CO_2 concentration under different velocity ranges of vehicular nodes.

We then observe the effect of different velocity ranges of vehicular nodes on the average GSM cost and the estimated error, as shown in Fig. 4. The velocity ranges of vehicular nodes are set to [5,25], [35,55], [65,85], [95,115], and [125,145] km/hr (kilometers per hour). It can be observed that the velocities of vehicular nodes has insignificant effects on both the GSM cost and the estimated error, especially when vehicular nodes move with higher velocities ($\geq$ 35 km/hr). Note that when vehicular nodes move with very low velocities (for example, 5 km/hr $\sim$ 25 km/hr), the effect of mobility could degrade and each node may only obtain data from few positions in the monitoring region. In this case, the estimated error will increase. From Fig. 4, the variation-based and gradient-based schemes can reduce both the GSM cost and the estimated error, compared with other schemes.

Fig. 5 shows the effect of different sizes of the monitored region on the average GSM cost and the estimated error. The region area is ranged from 6.4 km × 6.4 km to 102.4 km × 102.4 km. Changing the region size has almost no effect on the number of received messages, because the number of vehicular nodes is the same. However, the estimated error increases significantly when the region size increases, because the node density drops fast. From Fig. 5, it can be observed that our variation-based and gradient-based schemes can reduce both the GSM cost and the estimated error under different region sizes.

We then observe the effect of different numbers of streets on the average GSM cost and the estimated error, as shown in Fig. 6. The street number is ranged from 10 to 100. Changing the street number has almost no effect on the number of received messages (and thus the GSM cost), because the number

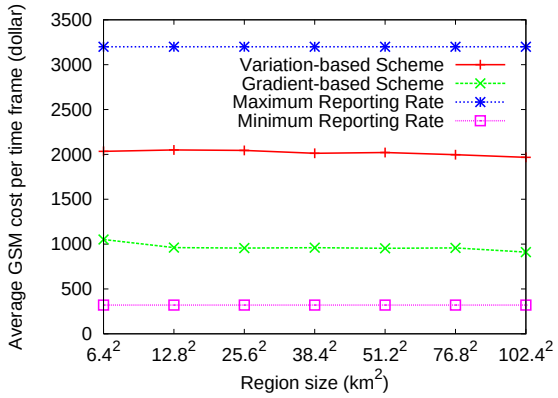

(a) GSM cost

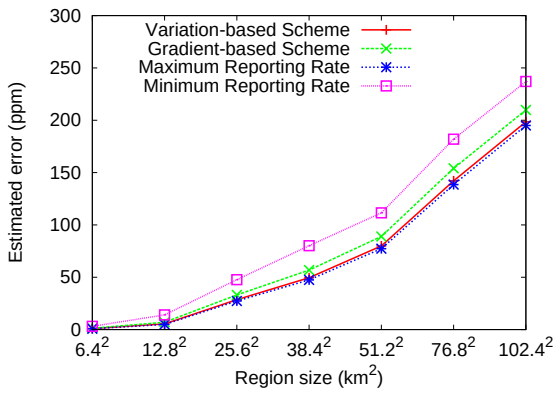

(b) estimated error

Fig. 5: Comparison of the GSM short message cost per time frame T and the estimated error of the CO_2 concentration under different sizes of the monitored region.

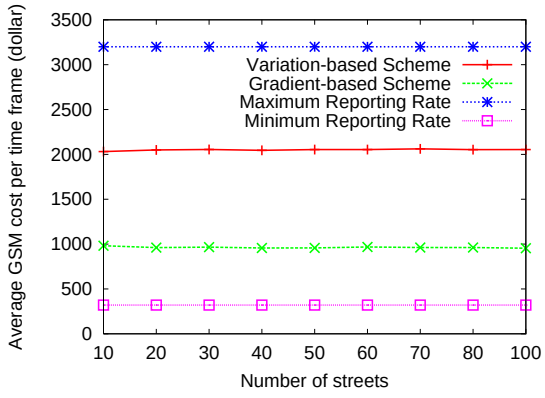

(a) GSM cost

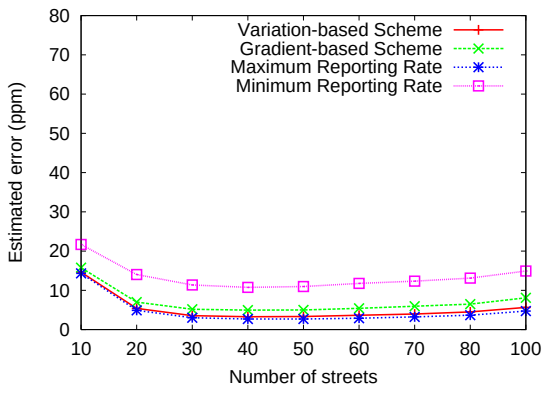

(b) estimated error

Fig. 6: Comparison of the GSM short message cost per time frame T and the estimated error of the CO_2 concentration under different numbers of streets.

of vehicular nodes does not change. When there are very few streets (for example, 10), vehicular nodes could obtain data from very sparse positions, which results in a higher estimated error. Our variation-based and gradient-based schemes have smaller GSM costs and estimated errors compared with other schemes under different numbers of streets.

From Figs. 5 and 6, we observe that the node density significantly affects the estimated error. According to different sizes and numbers of streets in the monitored regions, we can properly divide the region so that the node density of each grid is balanced. In this way, we can reduce the estimated error.

Fig. 7 shows the effect of different variations of the CO_2 concentration (in term of the number of CO_2 events) on the average GSM cost and the estimated error. We range the CO_2 events from 4 to 24 in every 600 seconds (i.e., the length of T). Because the number of vehicular nodes is constant, changing the CO_2 variation has almost no effect on the GSM cost. Interestingly, the GSM cost of the variation-based scheme suddenly drops when there are 8 CO_2 events. The reason is that the CO_2 variation in the experiment may not be significant so that smaller reporting rates are set in the variation-based scheme. On the contrary, CO_2 variation has significantly impact on the estimated error. In particular, since vehicular nodes report (almost) a constant amount of messages, increasing the CO_2 variation will result in a higher estimated error. However, both the variation-based and gradient-based schemes can keep quite low estimated errors while reducing the GSM costs.

Fig. 8 shows the effect of different time frames T on the average GSM cost and the estimated error. We range T from 300 to 1050 seconds. Explicitly, the number of received messages (and therefore the GSM cost) increases while the estimated error decreases when T increases. Such trends are more significant in the scheme of maximum reporting rate and the variation-based scheme. By adopting the gradient concept, the increase of the GSM cost of the gradient-based scheme is small (compared to the variation-based scheme). From Fig. 8, we suggest setting T to 600 seconds since it can obtain a certain degree of monitoring accuracy with the expenditure of reasonable GSM costs in our proposed schemes.

5 Prototyping Experiences

We have implemented a 16-vehicle prototypes to collect the CO_2 concentration in the Hsinchu City, Taiwan, where over 100,000 people commute daily to work. Therefore, the CO_2 concentration varies drastically. Each vehicle is equipped with the following hardware components (as shown in Fig. 9):

1) Jennic board: It is a microprocessor composed of a wireless communication module. Each Jennic board contains a JN5139 chip [23], which has a 32-bit RISC (reduced instruction set computing) processor, a fully-compliant 2.4 GHz IEEE 802.15.4 [24] transceiver, 192 KB of ROM, and 96 KB of RAM. We adopt the ZigBee protocol [25] for inter-board communication.
2) GPS receiver: We adopt the uPatch300 GPS module [26], which provides geographic locations with the maximum tolerant error of 1.8 meters. In our prototype, we set the reporting rate to one second.

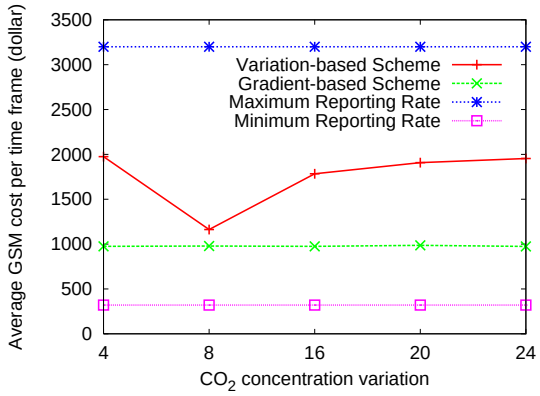

(a) GSM cost

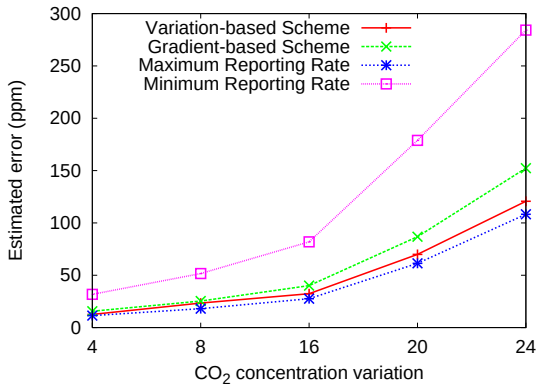

(b) estimated error

Fig. 7: Comparison of the GSM short message cost per time frame T and the estimated error of CO_2 concentration under different variations of the CO_2 concentration.

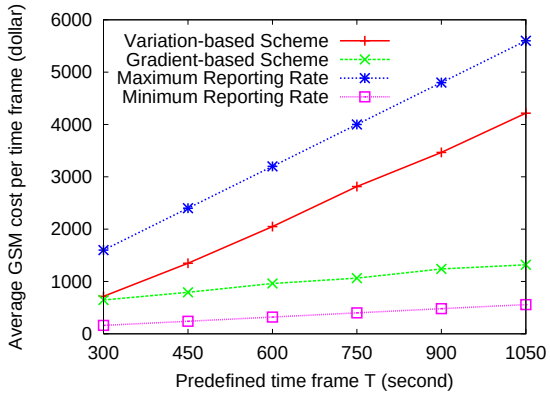

(a) GSM cost

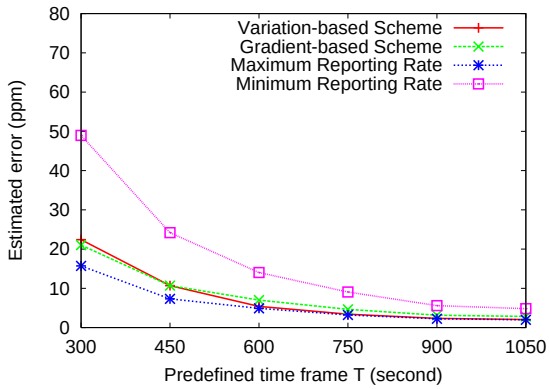

(b) estimated error

Fig. 8: Comparison of the GSM short message cost per time frame T and the estimated error of the CO_2 concentration under different T values.

3) CO_2 sensor: We adopt the H-550EV CO_2 sensor module [27], which samples the CO_2 concentration every three seconds. Its detectable range is from 0 to 5,000 ppm with an error range of ± 30 ppm, and has a response time of 30 seconds.
4) GSM module: We adopt the SIM300 GSM module [28], which supports the triband GSM/GPRS communication on frequency bands of 900 MHz, 1,800 MHz, and 1,900 MHz. It also allows users to transmit GSM short messages.

Fig. 9 shows the snapshots of the above components. The CO_2 sensor is installed outside the vehicle, while the GPS receiver and the GSM module are installed inside the vehicle. Each of the GPS receiver and the CO_2 sensor is attached to a Jennic board, so they can communicate with each other through a ZigBee wireless link. The GPS receiver is connected to the GSM module through an RS232 wired interface. The CO_2 sensor reports its readings at a fixed rate to the Jennic board inside the vehicle. The Jennic board will then average these readings, combine them with the current location of the vehicle, and report to the monitoring server through GSM short messages. The reporting behavior will follow the requested rate.

Each vehicle reports its current location and monitoring CO_2 concentration through a GSM short message, which follows the format of "time, CO_2 reading, latitude, longitude", as shown in Fig. 10. For example, a GSM short message of "18401300070002478.8722N12099.8483E" means that a vehicle has detected the CO_2 concentration of 700 ppm on the

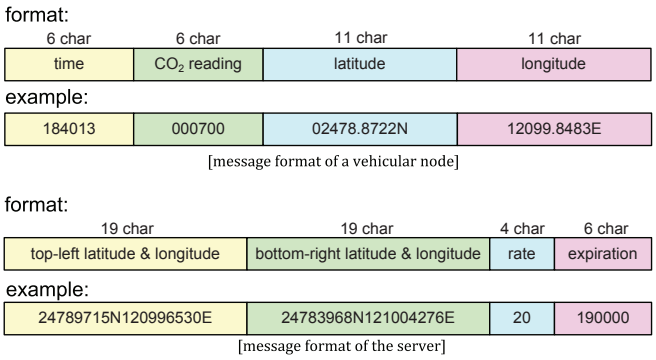

Fig. 10: The formats of our GSM short messages.

location of 2478.8722 degrees north latitude and 12099.8483 degrees east longitude at time 18:40:13 (hour:minute:second). On the other hand, the server can adjust the reporting rates of vehicles in certain region by sending a GSM message with the format of "latitude and longitude of the top-left point, latitude and longitude of the bottom-right point, new reporting rate, expiration time". For example, a GSM short message of "24789715N120996530E24783968N121
004276E20190000" means that the reporting rates of vehicles inside the rectangle with the top-left point at location (2478.9715N, 12099.6530E) and the bottom-right point at location (2440.8565N, 12100.4276E) should be adjusted to 20 times per hour, and this command will expire at time 19:00:00. The message format of the server is shown in Fig. 10.

Fig. 11 demonstrates our monitoring results in the Hsinchu City, Taiwan. The monitored region is approximately 160

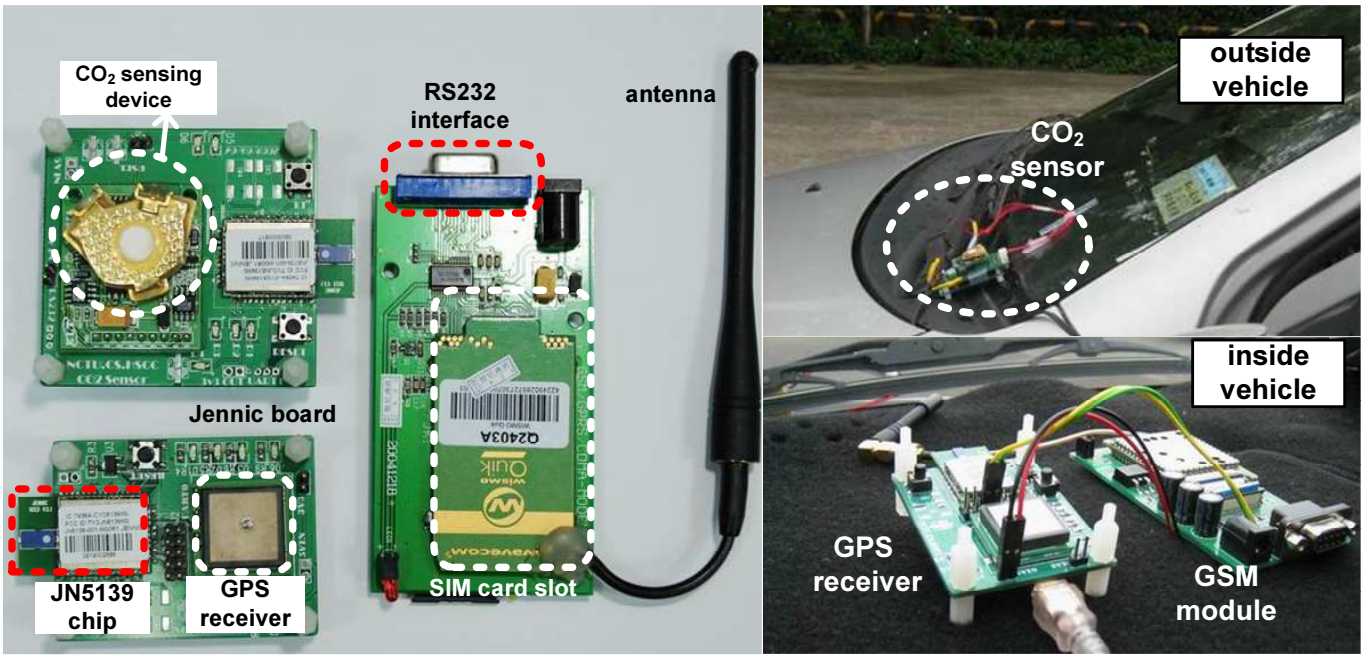

Fig. 9: The snapshots of hardware components in our prototype.

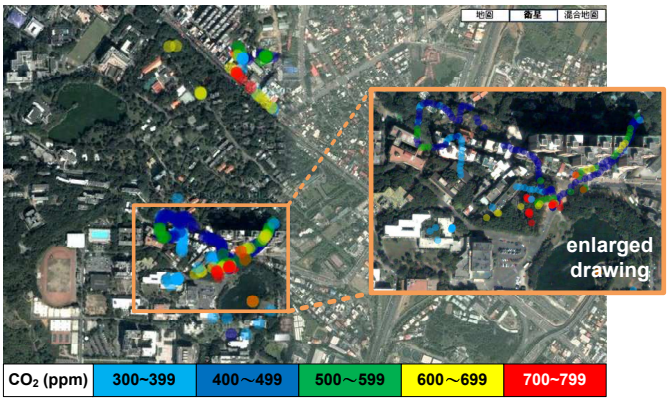

Fig. 11: A snapshot of the CO_2 concentration in the Hsinchu City, Taiwan.

hectares and is partitioned into 4×4 grids. The time frame T is set to 600 seconds. We use the Google Maps as the user interface. The observed CO_2 concentration ranges from 300 ppm to 800 ppm. Each circle in Fig. 11 indicates the monitoring position and its color represents the corresponding level of CO_2 concentration.

6 Conclusions

In this paper, we have proposed a new architecture based on VSNs for micro-climate monitoring. Through GSM short messages and geographic locations of vehicles, we can use a small number of vehicles to realize a fine-grained monitoring in city areas. To balance between the monitoring quality and the message cost, we have designed an adaptive approach to adjust the reporting rates of vehicular sensors according to the variance of sensing readings and the number of vehicular sensors in each grid. We have conducted some simulations to validate our proposed schemes, and also demonstrated the prototype of a ZigBee-based intra-vehicle wireless network for the micro-climate monitoring application.

References

[1] Google Maps. [Online]. Available: http://maps.google.com/
[2] T. He, S. Krishnamurthy, J.A. Stankovic, T. Abdelzaher, L. Luo, R. Stoleru, T. Yan, L. Gu, G. Zhou, J. Hui, and B. Krogh, "VigilNet: an integrated sensor network system for energy-efficient surveillance," *ACM Trans. Sensor Networks*, vol. 2, no. 1, pp. 1–38, 2006.
[3] K. Liu, M. Li, Y. Liu, M. Li, Z. Guo, and F. Hong, "Passive diagnosis for wireless sensor networks," *Proc. ACM Int'l Conf. Embedded Networked Sensor Systems*, 2008, pp. 113–126.
[4] M. Li and Y. Liu, "Underground structure monitoring with wireless sensor networks," *Proc. IEEE Int'l Symp. Information Processing in Sensor Networks*, 2007, pp. 69–78.
[5] G. Werner-Allen, J. Johnson, M. Ruiz, J. Lees, and M. Welsh, "Monitoring volcanic eruptions with a wireless sensor network," *Proc. European Workshop on Wireless Sensor Networks*, 2005, pp. 108–120.
[6] G. Werner-Allen, K. Lorincz, M. Ruiz, O. Marcillo, J. Johnson, J. Lees, and M. Welsh, "Deploying a wireless sensor network on an active volcano," *IEEE Internet Computing*, vol. 10, pp. 18–25, 2006.
[7] N. Xu, S. Rangwala, K.K. Chintalapudi, D. Ganesan, A. Broad, R. Govindan, and D. Estrin, "A wireless sensor network for structural monitoring," *Proc. ACM Int'l Conf. Embedded Networked Sensor Systems*, 2004, pp. 13–24.
[8] K. Chebrolu, B. Raman, N. Mishra, P.K. Valiveti, and R. Kumar, "Brimon: a sensor network system for railway bridge monitoring," *Proc. ACM Int'l Conf. Mobile systems, Applications, and Services*, 2008, pp. 2–14.
[9] H. Wang, D. Estrin, and L. Girod, "Preprocessing in a tiered sensor network for habitat monitoring," *EURASIP J. Applied Signal Processing*, 2003, pp. 392–401.
[10] K. Chebrolu, B. Raman, N. Mishra, P.K. Valiveti, and R. Kumar, "Luster: wireless sensor network for environmental research," *Proc. ACM Int'l Conf. Embedded Networked Sensor Systems*, 2007, pp. 103–116.
[11] G. Cao, G. Kesidis, T.L. Porta, B. Yao, and S. Phoha, "Purposeful mobility in tactical sensor networks," *Sensor Network Operations*, 2006.
[12] Y.C. Wang, F.J. Wu, and Y.C. Tseng, "Mobility management algorithms and applications for mobile sensor networks," *Wireless Comm. and Mobile Computing*, 2010.
[13] Y.C. Tseng, Y.C. Wang, K.Y. Cheng, and Y.Y. Hsieh, "iMouse: an integrated mobile surveillance and wireless sensor system," *Computer*, vol. 40, no. 6, pp. 60–66, 2007.
[14] J. Allred, A.B. Hasan, S. Panichsakul, W. Pisano, P. Gray, J. Huang, R. Han, D. Lawrence, and K. Mohseni, "Sensorflock: an airborne wireless sensor network of micro-air vehicles," *Proc. ACM Int'l Conf. Embedded Networked Sensor Systems*, 2007, pp. 117–129.
[15] P. Juang, H. Oki, Y. Wang, M. Martonosi, L. Peh, and D. Rubenstein, "Energy-efficient computing for wildlife tracking: design tradeoffs

and early experiences with zebranet," *ACM SIGOPS Operating Systems Review*, vol. 36, no. 5, pp. 96–107, 2002.
[16] S.B. Eisenman, E. Miluzzo, N.D. Lane, R.A. Peterson, G.S. Ahn, and A.T. Campbell, "Bikenet: A mobile sensing system for cyclist experience mapping," *ACM Trans. Sensor Networks*, vol. 6, pp. 1–39, 2009.
[17] H. Kargupta, R. Bhargava, K. Liu, M. Powers, P. Blair, S. Bushra, J. Dull, K. Sarkar, M. Klein, M. Vasa, and D. Handy, "VEDAS: a mobile and distributed data stream mining system for real-time vehicle monitoring," *Proc. SIAM Int'l Conf. Data Mining*, 2004, pp. 300–311.
[18] U. Lee, B. Zhou, M. Gerla, E. Magistretti, P. Bellavista, and A. Corradi, "Mobeyes: smart mobs for urban monitoring with a vehicular sensor network," *IEEE Wireless Comm.*, vol. 13, no. 5, pp. 52–57, 2006.
[19] B. Hull, V. Bychkovsky, Y. Zhang, K. Chen, M. Goraczko, A. Miu, E. Shih, H. Balakrishnan, and S. Madden, "Cartel: A distributed mobile sensor computing system," *Proc. ACM Int'l Conf. Embedded Networked Sensor Systems*, 2006, pp. 125–138.
[20] J.P. Sheu, P.C. Chen, and C.S. Hsu, "A distributed localization scheme for wireless sensor networks with improved grid-scan and vector-based refinement," *IEEE Trans. Mobile Computing*, vol. 7, no. 9, pp. 1110–1123, Sept. 2008.
[21] A. Gopakumar and L. Jocob, "Localization in wireless sensor networks using particle swarm optimization," *IET Int'l Conf. Wireless, Mobile and Multimedia Networks*, pp. 227–230, Jan. 2008.
[22] F. Bai, N. Sadagopan, and A. Helmy, "Important: a framework to systematically analyze the impact of mobility on performance of routing protocols for adhoc networks," *Proc. IEEE INFOCOM*, 2003, pp. 825–835.
[23] Jennic Wireless Microcontrollers. [Online]. Available: http://www.jennic.com/
[24] "IEEE standard for information technology—telecommunications and information exchange between systems—local and metropolitan area networks specific requirements part 15.4: wireless medium access control (MAC) and physical layer (PHY) specifications for low-rate wireless personal area networks (LR-WPANs)," 2006.
[25] "ZigBee specification version 2006, ZigBee document 064112," 2006.
[26] uPatch300 module. [Online]. Available: http://www.fastraxgps.com/
[27] H-550EV module. [Online]. Available: http://www.elti.co.kr/
[28] SIM300 module. [Online]. Available: http://www.sim.com/